International Journal of Coal Science & Technology (2022) 9:4
https://doi.org/10.1007/s40789-022-00470-8

RESEARCH

A highly active and stable $Sr_2Fe_{1.5}Mo_{0.5}O_{6-\delta}$-$Ce_{0.8}Sm_{0.2}O_{1.95}$ ceramic fuel electrode for efficient hydrogen production via a steam electrolyzer without safe gas

Yao Wang[1] · Tong Liu[1]

Received: 19 January 2021 / Accepted: 17 January 2022

Abstract
High temperature steam (H_2O) electrolysis via a solid oxide electrolysis cell is an efficient way to produce hydrogen (H_2) because of its high energy conversion efficiency as well as simple and green process, especially when the electrolysis process is combined with integrated gasification fuel cell technology or derived by renewable energy. However, about 60%–70% of the electricity input is consumed to overcome the large oxygen potential gradient but not for electrolysis to split H_2O to produce H_2 due to the addition of safe gas such as H_2 in the fuel electrode. In this work, $Sr_2Fe_{1.5}Mo_{0.5}O_{6-\delta}$-$Ce_{0.8}Sm_{0.2}O_{1.95}$ (SFM-SDC) ceramic composite material has been developed as fuel electrode to avoid the use of safe gas, and the open circuit voltage (OCV) has been effectively lowered from 1030 to 78 mV when the feeding gas in the fuel electrode is shifted from 3%H_2O–97%H_2 to 3%H_2O–97%N_2, reasonably resulting in a significantly increased electrolysis efficiency. In addition, it is also demonstrated that the electrolysis current density is greatly enhanced by increasing the humidity in the fuel electrode and the working temperature. A considerable electrolysis current density of −0.54 A/cm^2 is obtained at 800 °C and 0.4 V for the symmetrical electrolyzer by exposing SFM-SDC fuel electrode to 23%H_2O–77%N_2, and durability test at 800 °C for 35 h demonstrates a relatively stable electrochemical performance for steam electrolysis under the same operation condition without safe gas and a constant electrolysis current density of −0.060 A/cm^2. Our findings achieved in this work indicate that SFM-SDC is a highly promising fuel electrode for steam electrolysis.

Keywords Solid oxide electrolysis cell · Steam electrolysis · Fuel electrode · Molybdenum doped strontium ferrite · Safe gas

1 Introduction

The integrated gasification fuel cell (IGFC) system, which combines the coal gasification and solid oxide fuel cells (SOFCs), has been considered as one of the most promising technologies in the coal utilization for power generation because of superior electrical efficiency and efficient carbon dioxide capture and sequestration (CCS) (Lanzini et al. 2014; Li et al. 2014; Wang et al. 2020a). However, because of the high rate of greenhouse gas emissions, alternative technology is being sought to further reduce the environmental impact with coal utilization. Recently, hydrogen is regarded as an alternative candidate for future fuels because it can efficiently address the environmental and energy security issues associated with fossil-derived hydrocarbon fuels (Shoko et al. 2006; Wang et al. 2014). Among many hydrogen production methods, high-temperature steam electrolysis via a solid oxide electrolysis cell (SOEC), which is capable of producing zero-emission hydrogen if used in conjunction with IGFC technology or other renewable energies, is considered as one of the most promising alternative techniques for the hydrogen production from electricity due to its high efficiency and flexibility (Fan and Han 2014; Herring et al. 2007; Wang et al. 2014). It is well-known that a SOEC is actually a concentration cell, which is strongly associated with the gas conditions (partial oxygen pressure, p_{O2}) in both electrode sides. For the state-of-the-art Ni-based cathode in a steam electrolyzer, safe gas, such as hydrogen (H_2), is always fed to maintain the reduced atmosphere for

✉ Tong Liu
liu_tong@whu.edu.cn

[1] Key Laboratory of Hydraulic Machinery Transients, Ministry of Education, School of Power and Mechanical Engineering, Wuhan University, Hubei 430072 Wuhan, China

Published online: 21 February 2022

the prevention of nickel oxidation to nickel oxide (Bi et al. 2014; Liu et al. 2015; Wang et al. 2020b, 2017; Yang et al. 2021; Zheng et al. 2017). Meanwhile, the anode is typically exposed to air, and the by-product O_2 is normally wasted. To make things worse, p_{O2} in the anode side will continue to increase because of the accumulated O_2 generated during the electrolysis process, leading to a large p_{O2} difference between the two electrodes. This large oxygen gradient could produce a high open-circuit voltage (OCV) normally up to 1.1 V, which can be calculated using the Nernst equation. Since an applied voltage higher than OCV must be supplied in order to pump oxygen from the cathode side to the anode side during the electrolysis process, about 60%–70% of the electricity input is consumed to overcome the large oxygen potential gradient but not for electrolysis to split H_2O to produce H_2, resulting in a large amount electricity consumption and thus high operating or running cost, finally producing H_2 with low energy conversion efficiency. Therefore, it is highly desired to develop the steam electrolyzer without the addition of safe gas, which can be theoretically achieved by using noble metals or stable ceramic electrodes against H_2O, H_2 and their mixture at the elevated temperature.

In recent years, ceramic fuel electrodes such as $Sr_2Fe_{1.5}Mo_{0.5}O_{6-\delta}$ (SFM) (Li et al. 2017a, 2017b, 2019; Liu et al. 2010b, 2019; Wang et al. 2016a; Yang et al. 2019), $La_{0.75}Sr_{0.25}Cr_{0.5}Mn_{0.5}O_3$ (LSCM) (Kwon et al. 2019; Lu et al. 2018; Xing et al. 2015; Zhang et al. 2018), $La_xSr_{1-x}TiO_3$ (LST) (Li et al. 2012; Qi et al. 2014; Wu et al. 2020; Yaremchenko et al. 2020), $Sr_2MgMoO_{6-\delta}$ (Huang et al. 2006), $La_{0.8}Sr_{0.2}FeO_{3-\delta}$ (Li et al. 2020), $Sr_2(Fe,Ni,Mo)O_6$ (Du et al. 2016; Liu et al. 2020; Lv et al. 2019; Meng et al. 2020; Wang et al. 2018, 2016b) and $PrBaMnO_{5+\delta}$ (Sengodan et al. 2015; Zhu et al. 2019) have been intensively developed as the more redox stable fuel electrodes than classical Ni-based fuel electrodes for solid oxide cells. However, only a fewer fuel electrode materials have been used as the alternative electrodes to avoid the use of reducing gas as a safe gas during the operation (Li et al. 2017b; Torrell et al. 2015; Xie et al. 2011). But it is reported that the electrochemical performance of the fuel electrodes including LSCM and LST fuel electrodes were much lower than those of the classical Ni-based fuel electrodes (Torrell et al. 2015; Xie et al. 2011). On the contrast, SFM fuel electrode demonstrated comparative electrochemical performance when operated under co-electrolysis conditions without using the safe gas (Li et al. 2017b).

Recently, SFM material, which has been successfully used as both oxygen electrode and hydrogen electrode for solid oxide cells (Li et al. 2017a, b, 2019; Liu et al. 2010a, b, 2019; Skubida et al. 2021; Wang et al. 2016a; Zheng et al. 2015), is proven to be a promising alternative electrode material because of its high catalytic activity, high electrical conductivity in both reducing and oxidizing atmosphere, and excellent redox stability. However, no attention has been focused on the hydrogen production by using SFM electrode via the steam electrolysis process without safe gas. In the present work, we try to explore electrochemical characterization of such symmetrical solid oxide electrolysis cell with SFM electrodes operated without the existence of reduced gas in the SFM fuel electrode side.

Symmetrical electrolyzers with a cell configuration of 60wt% SFM-40wt% $Sm_{0.2}Ce_{0.8}O_{1.9}$ (SFM-SDC)/$La_{0.80}Sr_{0.20}Ga_{0.80}Mg_{0.20}O_{3-\delta}$ (LSGM)/SFM-SDC are prepared for steam electrolysis application, and nitrogen gas instead of hydrogen gas is used as carrier gas, trying to reduce the partial oxygen pressure difference between the two electrodes (SFM oxygen electrode and SFM fuel electrode), and expecting a lower thermal-dynamic barrier and much improved energy conversion efficiency.

2 Experimental

The electrode materials including SFM and SDC powders were synthesized using the citric-assisted combustion method (Wang et al. 2016a), while the LSGM powders were purchased from FuelCellMaterials Inc. Dense LSGM electrolyte were fabricated by pressing the LSGM powders to pellets and sintering at 1400 °C for 5 h. SFM-SDC ink with a weight ratio of 60:40 was screen-printed on both sides of the electrolyte and then sintering at 1050 °C for 2 h to form SFM-SDC/LSGM/SFM-SDC symmetrical cells for steam electrolysis application. Finally, gold (Au) paste was screen-printed on SFM-SDC electrodes and calcined at 800 °C for 1 h. The effective cell area was measured to be 0.33 cm^2. Note that the thickness of LSGM electrolyte is about 500 mm, while the thickness of the SFM-SDC electrode is about 30 mm.

The morphology of the fuel electrode after testing was examined by using a scanning electron microscope (SEM, Tescan MIRA 3).

Cell tests were performed at a home-made setup, and the details were described in our previous work (Liu et al. 2019). Mass flow rates of N_2 and H_2 gases in the fuel electrode side were precisely controlled by using digital mass flow controller (MC-100SCCM-D/5M, Alicat Scitific Inc), while water vapor was added to the gas stream via a humidifier by heating liquid water to a certain temperature, and the steam content was measured by using a humidity sensor (HTM 338, Vasala). Electrochemical performance including current density-cell voltage (*i-V*), electrochemical impedance spectra (EIS) and short-term durability were carried out by using an electrochemical workstation (Versa STAT 3–400 test system, Princeton Applied Research Inc). The *i-V* curves for steam electrolyzers with and without safe gas (H_2) were recorded from OCV to 1.5 V and OCV to 0.4 V

with a voltage sweeping speed of 0.03 V/s, respectively. EIS under both the OCV and steam electrolysis with a constant current density of −0.060 A/cm^2 conditions were collected with a voltage amplitude of 0.03 V in the frequency range of 10^6–10^{-2} Hz.

3 Results and discussion

Figure 1 shows the *i-V* curves measured at 800 °C for the symmetrical SFM-SDC/LSGM/SFM-SDC electrolysis cell operating its cathode in 3% H_2O humidified N_2 and H_2, respectively. It can be clearly seen that the *i-V* curve preformed in 3% H_2O humidified N_2 atmosphere is far below that for the conventional solid oxide steam electrolyzer operated in 3% H_2O humidified H_2 atmosphere, indicating that a much lower applied potential is required to produce the same amount of electrolysis current and hydrogen gas. For instance, the cell voltage to produce electrolysis current density of −0.100 A/cm is 1.1 V for the conventional steam electrolysis with the cathode and anode exposed to 3%H_2O–97%H_2 and ambient air, respectively; while the applied cell voltage has decreased nearly one order of magnitude to 0.3 V when the feeding gas in the cathode side is changed to 3%H_2O–97%N_2. These results demonstrate that it really promotes the electrolysis efficiency on the symmetrical SFM-SDC/LSGM/SFM-SDC electrolysis cell by the substitution of the cathode atmosphere with humidified N_2 due to the dramatic decrease of the applied potential.

Another obvious evidence for such enhancement is from the OCV data for symmetrical electrolyzer operated in different cathode atmospheres at 700–800 °C. As obviously shown in Fig. 1 and Table 1 that the OCV values for the

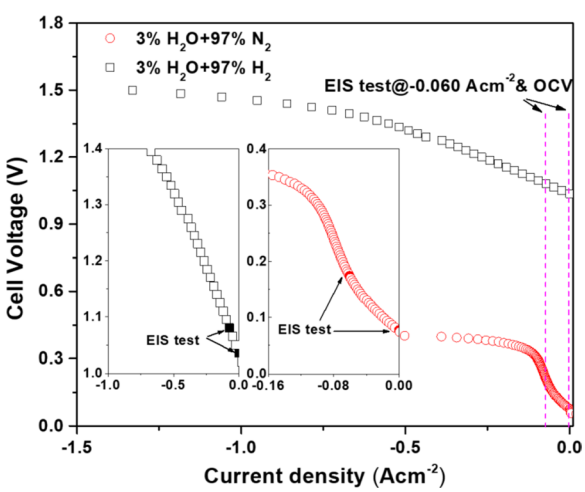

Fig. 1 *i-V* curves measured at 800 °C for the symmetrical SFM-SDC/LSGM/SFM-SDC electrolysis cell operating its cathode in 3%H_2O humidified N_2 (red circle) and H_2 (black square), respectively

Table 1 Measured OCV data for symmetrical cell with a cell configuration of SFM-SDC/LSGM/SFM-SDC in different cathode atmosphere at 700, 750 and 800 °C

Gas atmosphere	OCV (mV)		
	700 °C	750 °C	800 °C
3%H_2O–97%N_2	54	60	78
10%H_2O–90%N_2	54	60	73
23% H_2O–77%N_2	50	55	66
33% H_2O–67%N_2	48	53	65
3% H_2O–97% H_2	1060	–	1030

symmetrical cell, which indicates the cell voltage corresponds to zero electrolysis current (density), are remarkably dropped from 1030 and 1060 mV for conventional steam electrolysis to 78 and 54 mV when the sweeping gas in the cathode side is shifted from 3%H_2O–97%H_2 to 3%H_2O–97%N_2, respectively. In addition, the OCV data at different H_2O-N_2 mixtures are also measured, and summarized in Table 1. It is clearly demonstrated that when the cathode side is fed with H_2O-N_2 mixture, the OCV data are all located at the voltage range of 48–78 mV, which are significantly lower than the theoretical Nernst potential for H_2O-H_2 mixtures (approx. 1.0 V) (Chen and Jiang 2020), which demonstrates much less energy barrier needs to be overcome to yield the electrolysis reaction when inert N_2 instead of safe gas H_2 is used as carrier gas. Meanwhile, it is shown that a slight decrease in OCV was obtained with lowering the operating temperature, which could be explained by the lowered theoretical OCV calculated by Nernst equation

$$V_{\text{Nernst}} = \frac{RT}{4F} \ln \frac{p_{O_2,\text{anode}}}{p_{O_2,\text{cathode}}} \quad (1)$$

where R is the universal gas constant, T is the absolute operating temperature, F is the Faraday constant, $p_{O_2,\text{anode}}$ and $p_{O_2,\text{cathode}}$ are the oxygen partial pressure of the air and N_2-H_2O atmosphere in the anode and cathode chamber, respectively.

It is well known that the electrolysis reaction mechanism is greatly affected by the electrode operating conditions, such as feeding gas composition, applied voltage (Bi et al. 2014; Liu et al. 2015; Wang et al. 2017; Zheng et al. 2017). Therefore, the electrochemical reactions and corresponding rate-determining steps in humidified H_2 and N_2 conditions may be quite different, which can be obviously expressed by the different slopes in the *i-V* curves (Fig. 1). At the same time, the electrochemical impedance spectra (EIS) at OCV and −0.060 A/cm^2 conditions are collected and then fitted by using Z-View software. As shown in Fig. 2, the impedance spectra show good agreement with

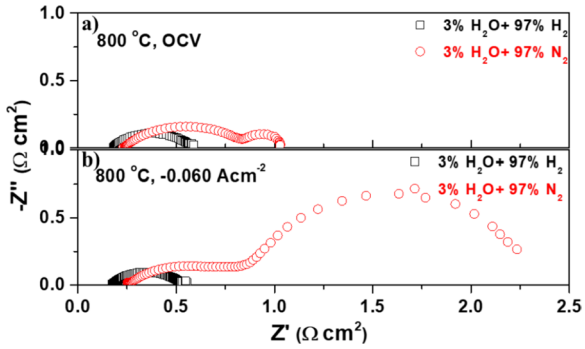

Fig. 2 Electrochemical impedance spectra recorded at 800 °C for SFM-SDC/LSGM/SFM-SDC symmetrical cell operated at **a** OCV and **b** −0.060 A/cm^2 with humidified N_2 and H_2 as the cathode gases, respectively

the equivalent circuit R_0 (R_iCPE_i), where R_0 is attributed to the resistance of the electrolyte; while (R_iCPE_i) is related to a sub-step in the electrochemical reaction process, and described as a depressed semi-circle in the Nyquist plots. When the cell is operated with humidified H_2, the impedance spectra measured at OCV are composed of only one arc with the typical frequency of 158 Hz. The resistance is 0.41 Ω cm^2 for the sub-step determining the total electrolysis reaction process. It is also noted that the impedance exhibits only a relatively weak dependence on current density, due to the similar shape and magnitude at 0 and −0.060 A/cm^2, which is highly consistent with the fact that the *i-V* curve is nearly linear within the whole range of applied potential from OCV to OCV + 0.25 V. While when the cell is operated with humidified N_2, the whole impedance spectra are composed of two arcs with an additional arc presenting at a lower frequency. And the contribution from the second arc to the total area specific resistance increases with increasing the electrolysis current density. As shown in Fig. 2a, the resistance of the low frequency arc (R_2) measured at OCV is 0.17 Ω cm^2, accounting for 21% of the total area specific resistance (R_p). The resistance magnitude and ratio has increased to 1.38 Ω cm^2 and 67% with increasing the electrolysis current density to −0.060 A/cm^2 (Fig. 2b), which are strongly consistent with the great increase of slope at high electrolysis current density (Table 2).

Figure 3a shows the he *i-V* curves measured at 800 °C for the symmetrical SFM-SDC/LSGM/SFM-SDC electrolysis cell operating its cathode in different humidified N_2 atmospheres (xH_2O-(1-x)N_2, x = 3%, 10%, 23%, and 33%). It is observed that the OCV value at 800 °C is slightly lowered from 78 mV to 73, 66, 65 mV when sweeping gas in the fuel electrode is changed from 3%H_2O–97%N_2 to 10%H_2O–90%N_2, 23%H_2O–77%N_2 and 33%H_2O–67%N_2, respectively. At the same time, it can be clearly seen that at the voltage lower than 0.3 V, the electrochemical

Table 2 The fitted electrode resistances shown in Fig. 2 for the SFM-SDC/LSGM/SFM-SDC symmetrical cell operated at 800 °C and exposed the fuel electrode to 3% H_2O Humidified H_2 and 3% H_2O Humidified N_2, respectively

Resistance (A/cm^2)	Working conditions			
	3%H_2O–97%H_2		3%H_2O–97%N_2	
	R_1 (Ω cm^2)	R_2 (Ω cm^2)	R_1 (Ω cm^2)	R_2 (Ω cm^2)
0 (OCV)	0.41	–	0.64	0.17
−0.060	0.36	–	0.69	1.38

performance is gradually enhanced with increasing the humidity, and the applied operating electrolysis voltage to generate an electrolysis current density of −0.060 A/cm^2 is continually decreased from 0.174 V to 0.154, 0.130, and 0.129 V as the feeding gas in the cathode is shifted from 3%H_2O–97%N_2 to 10%H_2O–90%N_2, 23%H_2O–77%N_2 and 33%H_2O–67%N_2, respectively. Additionally, it is also found that the electrolysis current density is greatly enhanced from −0.098 A/cm^2 to −0.108, −0.128 and −0.134 A/cm^2 as the

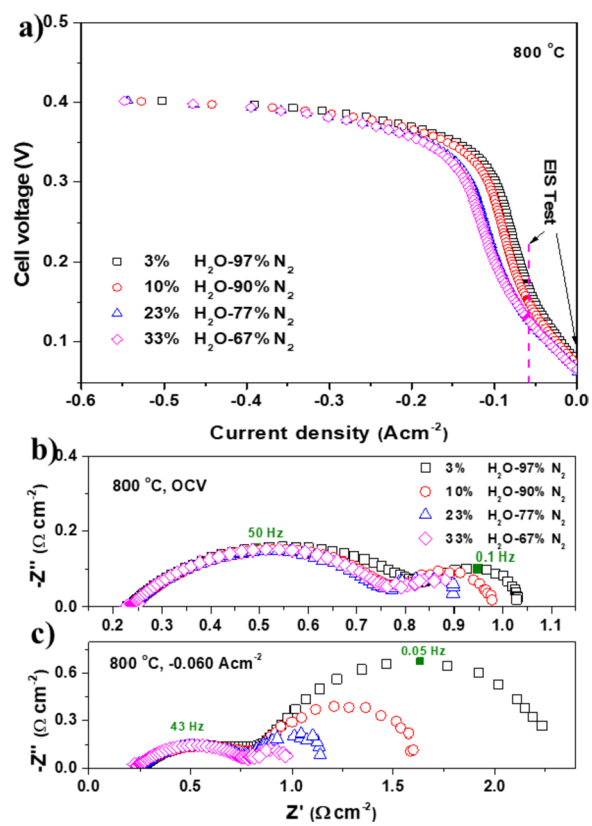

Fig. 3 **a** *i-V* curves and EIS measured at **b** OCV, and **c** −0.060 A/cm^2 conditions at 800 °C for symmetrical cell with a cell configuration of SFM-SDC/LSGM/SFM-SDC operated at different cathode atmosphere

steam content is increased from 3% to 10%, 23%, and 33%, respectively.

Electrochemical impedance spectra (EIS) under OCV and −0.060 A/cm^2 conditions at 800 °C are also measured to investigate the electrochemical performance of symmetrical electrolyzers operated at different steam contents, and the Nyquist plots of the impedance spectra measured under the OCV and −0.060 A/cm^2 conditions are in Fig. 3b and c, respectively. At OCV condition, as the steam content is raised from 3 to 33%, the total resistance (R_{total}) is gradually decreased from 1.04 to 0.90 Ω cm^2 while the ohmic resistance (R_{ohmic}) is almost stable with a value of about 0.23 Ω cm^2 (Fig. 3b). It is calculated that the electrode polarization resistance (R_p) at OCV condition is continually lowered from 0.81 to 0.67 Ω cm^2. Additionally, it is found that R_{total} is strongly decreased from 2.32 to 0.1.01 Ω cm^2 with a stable R_{ohmic} of 0.25 Ω cm^2 (Fig. 3c), leading to a greatly lowered R_p from 2.07 to 0.76 Ω cm^2 with increasing the humidity from 3% to 33%. To better understand the humidity effect on the electrode reaction, R_ps are fitted by using ZSimpleWin software and summarized in Table 3. It is found that R_1 values in the high frequency range are gradually decreased from 0.64 and 0.69 Ω cm^2 to 0.53 and 0.59 Ω cm^2 after gradually increasing the humidity from 3% to 33% when an electrolysis current density of 0 and −0.060 A/cm^2 is applied on the electrolyzer, respectively, which is possibly enhanced by the increased triple phase boundaries (TPBs) induced by the increased reactive gas H_2O in the SFM-SDC fuel electrode. However, different trends have been obtained for R_2 in the low frequency range, which is strongly associated with diffusion, adsorption, and dissociation of reactive gas (H_2O) in the electrode (Chen et al. 2020; Liu et al. 2020; Meng et al. 2020; Yan et al. 2020). No obvious variation has been observed at OCV condition (0.14–0.18 Ω cm^2) when the humidity is raised from 3% to 33%, which can be explained by the fact that no reactive gas has been consumed at OCV condition. On the contrast, the corresponding R_2 value is significantly decreased from 1.38 to 0.17 Ω cm^2 with increasing the steam content from 3% to 33%. In addition, R_p values as well as R_2 values measured at −0.060 A/cm^2 and low steam content conditions are much larger than those at OCV condition. These phenomena are possibly ascribed to the severe concentration resistance induced by the insufficient reactive gas at low humidity.

Table 3 The total polarization resistances shown in Fig. 3 for the SFM-SDC/LSGM/SFM-SDC symmetrical electrolyzer operated at 800 °C and measured at OCV and −0.060 A/cm^2 conditions

Gas atmosphere	Working conditions			
	OCV		−0.060 A/cm^2	
	R_1 (Ω cm^2)	R_2 (Ω cm^2)	R_1 (Ω cm^2)	R_2 (Ω cm^2)
3%H_2O–97%N_2	0.64	0.16	0.69	1.38
10%H_2O–90%N_2	0.58	0.18	0.65	0.73
23%H_2O–77%N_2	0.53	0.14	.0.59	0.32
33%H_2O–67%N_2	0.53	0.14	0.59	0.17

Figure 4a shows the he *i-V* curves recorded in the temperature range of 700–800 °C with an interval of 50 °C for the symmetrical SFM-SDC/LSGM/SFM-SDC electrolysis cell when the cathode and anode are exposed to 23%H_2O–77%N_2 and ambient air, respectively. As depicted in Fig. 4a, the electrolysis reaction can be effectively enhanced by increasing the operating temperature(Gui et al. 2020; Zhang et al. 2020). For example, the electrolysis current density is strongly increased from −0.23 to −0.39, and −0.54 A/cm^2 with increasing the working temperature from 700 to 750, and 800 °C at 0.4 V, respectively. At the same time, the corresponding applied cell voltage is gradually lowered from 0.19 to 0.15, and 0.14 V at the electrolysis current density of −0.060 A/cm^2 when the working temperature is raised from 700 to 750, and 800 °C, respectively. These phenomena can be explained by the fact that the electrode reaction process can be effectively accelerated by the increased oxygen ion conductivity and electro-catalytic properties of electrode materials at the elevated temperature, which can also be

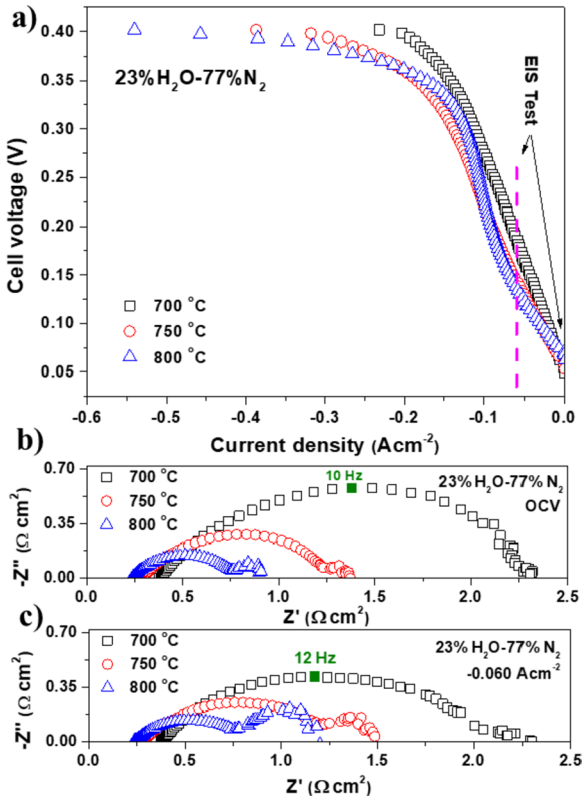

Fig. 4 **a** *i-V* curves and EIS measured at **b** OCV, and **c** −0.060 A/cm^2 conditions in the temperature range of 700–800 °C with an interval of 50 °C for symmetrical cell with a cell configuration of SFM-SDC/LSGM/SFM-SDC operated at 23%H_2O–77%N_2 condition

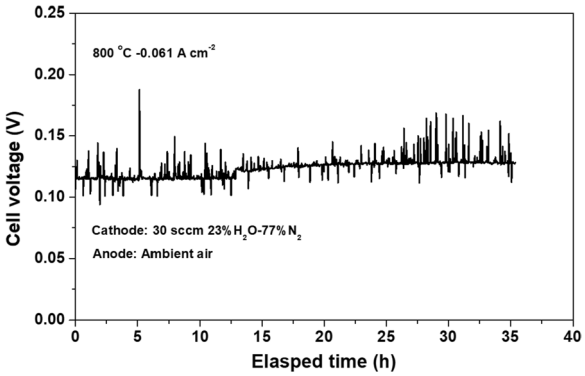

Fig. 5 The electrochemical performance durability results recorded at 800 °C and a constant electrolysis current density of −0.061 A/cm^2 with 23%H_2O–77%N_2 as the fuel and ambient air as the oxidant

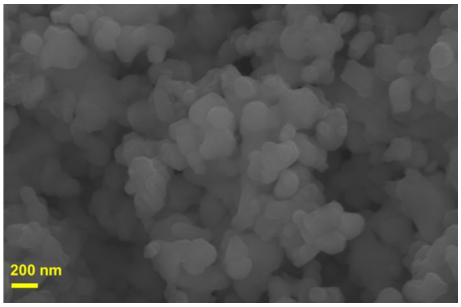

Fig. 6 SEM image of SFM-SDC fuel electrode after 35 h stability studies at 800 °C

confirmed by the decreased resistance for the steam electrolyzer. It is found from Fig. 4b that R_{total} and R_{ohmic} values collected at OCV condition are effectively decreased from 2.30 and 0.38 Ω cm^2 to 0.91 and 0.23 Ω cm^2, respectively, meaning that R_p value is strongly decreased from 1.92 to 0.68 Ω cm^2 with increasing the working temperature from 700 to 800 °C. Meanwhile, the effectively lowered R_{total}, R_{ohmic} and R_p values are also obtained at an electrolysis current density of −0.060 A/cm^2 condition (Fig. 4c), and the corresponding values are greatly lowered from 2.30, 0.38 and 1.92 Ω cm^2 to 1.20, 0.24 and 0.96 Ω cm^2, respectively. These results clearly demonstrate that the steam electrolysis reaction can be effectively accelerated by increasing the operating temperature.

Furthermore, it can be clearly seen from Fig. 5 that the symmetrical electrolyzer is almost stable at a constant electrolysis current density of −0.060 A/cm^2 in 35-h testing at 800 °C when the fuel electrode and oxygen electrode are exposed to 23%H_2O–77%N_2 and ambient air, respectively.

To further confirm the considerable stability, the microstructure of the electrolysis cell after the 35-h stability studies is shown in Fig. 6. When compared with fresh SFM-SDC electrode previously reported (Liu et al. 2019), no obvious change can be observed. These results obtained in this work indicate that SFM-SDC electrode is a great promising alternative fuel electrode and oxygen electrode for solid oxide electrolyzer based on LSGM electrolyte and safe gas free electrodes because of its good electrochemical performance and stability.

4 Conclusion

In this work, SFM-SDC composite electrodes have been prepared for both the fuel electrode and oxygen electrode. It is demonstrated that the steam electrolyzers with a cell configuration of SFM-SDC/LSGM/SFM-SDC can operate at the condition without safe gas, and strongly lower the cell voltage to produce hydrogen via steam electrolysis. In addition, these cells exhibit a considerable electrolysis current density and good durability during the operation. These results demonstrate that SFM-SDC ceramic electrode is a great promising alternative fuel electrode and oxygen electrode for solid oxide electrolyzer based on LSGM electrolyte and safe gas free electrodes because of its good electrochemical performance and stability. Our findings in this work can guide the development of ceramic electrode for solid oxide cells without safe gas.

Acknowledgements This work was supported by National Natural Science Foundation of China (51602228, 51502207).

Author's contribution TL and YW conducted the experimental, analyzed the experimental results and wrote the manuscript.

Declarations

Conflict of interests The authors declare that they have no known competing financial interests or personal relationships that could have appeared to influence the work reported in this paper.

References

Bi L, Boulfrad S, Traversa E (2014) Steam electrolysis by solid oxide electrolysis cells (soecs) with proton-conducting oxides. Chem Soc Rev 43:8255–8270. https://doi.org/10.1039/C4CS00194J

Chen K, Jiang SP (2020) Surface segregation in solid oxide cell oxygen electrodes: phenomena, mitigation strategies and electrochemical properties. Electrochem Energ Rev 3:730–765. https://doi.org/10.1007/s41918-020-00078-z

Chen Z, Jiang W, Lu Z, Wang Z, Chen Z, Jiang SP, Lin T, Shao Y, Tang D, Chen K, Ai N (2020) Accelerating effect of polarization on electrode/electrolyte interface generation and electrocatalytic performance of $Er_{0.4}Bi_{1.6}O_3$ decorated $Sm_{0.95}CoO_{3-\delta}$ cathodes. J Power Sources 465:228281. https://doi.org/10.1016/j.jpowsour.2020.228281

Du Z, Zhao H, Yi S, Xia Q, Gong Y, Zhang Y, Cheng X, Li Y, Gu L, Swierczek K (2016) High-performance anode material $Sr_2FeMo_{0.65}Ni_{0.35}O_{6-\delta}$ with in situ exsolved nanoparticle catalyst. ACS Nano 10:8660–8669. https://doi.org/10.1021/acsnano.6b03979

Fan H, Han M (2014) Electrochemical performance and stability of Sr-doped $LaMnO_3$-infiltrated yttria stabilized zirconia oxygen electrode for reversible solid oxide fuel cells. Int J Coal Sci Technol 1:56–61. https://doi.org/10.1007/s40789-014-0015-4

Gui L, Wang Z, Zhang K, He B, Liu Y, Zhou W, Xu J, Wang Q, Zhao L (2020) Oxygen vacancies-rich $Ce_{0.9}Gd_{0.1}O_{2-\delta}$ decorated $Pr_{0.5}Ba_{0.5}CoO_{3-\delta}$ bifunctional catalyst for efficient and long-lasting rechargeable Zn-air batteries. Appl Catal B-Environ 266:118656. https://doi.org/10.1016/j.apcatb.2020.118656

Herring JS, O'Brien JE, Stoots CM, Hawkes GL, Hartvigsen JJ, Shahnam M (2007) Progress in high-temperature electrolysis for hydrogen production using planar SOFC technology. Int J Hydrogen Energy 32:440–450. https://doi.org/10.1016/j.ijhydene.2006.06.061

Huang Y-H, Dass RI, Xing Z-L, Goodenough JB (2006) Double perovskites as anode materials for solid-oxide fuel cells. Science 312:254–257. https://doi.org/10.1126/science.1125877

Kwon Y, Yoo JY, Jang Y-h, Bae J (2019) Long-term durability of $La_{0.75}Sr_{0.25}Cr_{0.5}Mn_{0.5}O_3$ as a fuel electrode of solid oxide electrolysis cells for co-electrolysis. J CO2 Util 31:192–197. https://doi.org/10.1016/j.jcou.2019.03.004

Lanzini A, Kreutz TG, Martelli E, Santarelli M (2014) Energy and economic performance of novel integrated gasifier fuel cell (IGFC) cycles with carbon capture. Int J Greenh Gas Con 26:169–184. https://doi.org/10.1016/j.ijggc.2014.04.028

Li H, Yu Y, Han M, Lei Z (2014) Simulation of coal char gasification using O_2/CO_2. Int J Coal Sci Technol 1:81–87. https://doi.org/10.1007/s40789-014-0010-9

Li J, Fu Z, Wei B, Su C, Yue X, Lü Z (2020) Tailoring tantalum doping into a perovskite ferrite to obtain a highly active and stable anode for solid oxide fuel cells. J Mater Chem A 8:18778–18791. https://doi.org/10.1039/D0TA04857G

Li Y, Chen X, Yang Y, Jiang Y, Xia C (2017a) Mixed-conductor $Sr_2Fe_{1.5}Mo_{0.5}O_{6-\delta}$ as robust fuel electrode for pure CO_2 reduction in solid oxide electrolysis cell. ACS Sustain Chem Eng 5:11403–11412. https://doi.org/10.1021/acssuschemeng.7b02511

Li Y, Hu B, Xia C, Xu WQ, Lemmon JP, Chen F (2017b) A novel fuel electrode enabling direct CO_2 electrolysis with excellent and stable cell performance. J Mater Chem A 5:20833–20842. https://doi.org/10.1039/c7ta05750d

Li Y, Li Y, Wan Y, Xie Y, Zhu J, Pan H, Zheng X, Xia C (2019) Perovskite oxyfluoride electrode enabling direct electrolyzing carbon dioxide with excellent electrochemical performances. Adv Energy Mater 9:1803156. https://doi.org/10.1002/aenm.201803156

Li Y, Zhou J, Dong D, Wang Y, Jiang JZ, Xiang H, Xie K (2012) Composite fuel electrode $La_{0.2}Sr_{0.8}TiO_{3-\delta}$–$Ce_{0.8}Sm_{0.2}O_{2-\delta}$ for electrolysis of CO_2 in an oxygen-ion conducting solid oxide electrolyser. Phys Chem Chem Phys 14:15547–15553. https://doi.org/10.1039/C2CP42232H

Liu Q, Dong X, Xiao G, Zhao F, Chen F (2010a) A novel electrode material for symmetrical sofcs. Adv Mater 22:5478–5482. https://doi.org/10.1002/adma.201001044

Liu Q, Yang C, Dong X, Chen F (2010b) Perovskite $Sr_2Fe_{1.5}Mo_{0.5}O_{6-\delta}$ as electrode materials for symmetrical solid oxide electrolysis cells. Int J Hydrogen Energy 35:10039–10044. https://doi.org/10.1016/j.ijhydene.2010.08.016

Liu T, Liu H, Zhang X, Lei L, Zhang Y, Yuan Z, Chen F, Wang Y (2019) A robust solid oxide electrolyzer for highly efficient electrochemical reforming of methane and steam. J Mater Chem A 7:13550–13558. https://doi.org/10.1039/c9ta00467j

Liu T, Wang Y, Zhang Y, Fang S, Lei L, Ren C, Chen F (2015) Steam electrolysis in a solid oxide electrolysis cell fabricated by the phase-inversion tape casting method. Electrochem Commun 61:106–109. https://doi.org/10.1016/j.elecom.2015.10.015

Liu T, Zhao Y, Zhang X, Zhang H, Jiang G, Zhao W, Guo J, Chen F, Yan M, Zhang Y, Wang Y (2020) Robust redox-reversible perovskite type steam electrolyser electrode decorated with in situ exsolved metallic nanoparticles. J Mater Chem A 8:582–591. https://doi.org/10.1039/c9ta06309a

Lu J, Zhu C, Pan C, Lin W, Lemmon JP, Chen F, Li C, Xie K (2018) Highly efficient electrochemical reforming of CH_4–CO_2 in a solid oxide electrolyser. Sci Adv 4:eaar5100. https://doi.org/10.1126/sciadv.aar5100

Lv H, Lin L, Zhang X, Gao D, Song Y, Zhou Y, Liu Q, Wang G, Bao X (2019) In situ exsolved $FeNi_3$ nanoparticles on nickel doped $Sr_2Fe_{1.5}Mo_{0.5}O_{6-\delta}$ perovskite for efficient electrochemical CO_2 reduction reaction. J Mater Chem A 7:11967–11975. https://doi.org/10.1039/c9tǎ5d

Meng X, Wang Y, Zhao Y, Zhang T, Yu N, Chen X, Miao M, Liu T (2020) In-situ exsolution of nanoparticles from Ni substituted $Sr_2Fe_{1.5}Mo_{0.5}O_6$ perovskite oxides with different ni doping contents. Electrochim Acta 348:136351. https://doi.org/10.1016/j.electacta.2020.136351

Qi W, Gan Y, Yin D, Li Z, Wu G, Xie K, Wu Y (2014) Remarkable chemical adsorption of manganese-doped titanate for direct carbon dioxide electrolysis. J Mater Chem A 2:6904–6915. https://doi.org/10.1039/C4TA00344F

Sengodan S, Choi S, Jun A, Shin TH, Ju YW, Jeong HY, Shin J, Irvine JT, Kim G (2015) Layered oxygen-deficient double perovskite as an efficient and stable anode for direct hydrocarbon solid oxide fuel cells. Nat Mater 14:205–209. https://doi.org/10.1038/nmat4166

Shoko E, McLellan B, Dicks AL, da Costa JCD (2006) Hydrogen from coal: production and utilisation technologies. Int J Coal Geol 65:213–222. https://doi.org/10.1016/j.coal.2005.05.004

Skubida W, Zheng K, Stępień A, Świerczek K, Klimkowicz A (2021) $SrCe_{0.9}In_{0.1}O_{3-\delta}$-based reversible symmetrical protonic ceramic cell. Mater Res Bull 135:111154. https://doi.org/10.1016/j.materresbull.2020.111154

Torrell M, Garcia-Rodriguez S, Morata A, Penelas G, Tarancon A (2015) Co-electrolysis of steam and CO_2 in full-ceramic symmetrical soecs: a strategy for avoiding the use of hydrogen as a safe gas. Faraday Discuss 182:241–255. https://doi.org/10.1039/c5fd00018a

Wang F, Deng S, Zhang H, Wang J, Zhao J, Miao H, Yuan J, Yan J (2020a) A comprehensive review on high-temperature fuel cells with carbon capture. Appl Energ 275:115342. https://doi.org/10.1016/j.apenergy.2020.115342

Wang M, Wang Z, Gong X, Guo Z (2014) The intensification technologies to water electrolysis for hydrogen production—a review. Renew Sust Energ Rev 29:573–588. https://doi.org/10.1016/j.rser.2013.08.090

Wang X, Wei K, Yan S, Wu Y, Kang J, Feng P, Wang S, Zhou F, Ling Y (2020b) Efficient and stable conversion of oxygen-bearing low-concentration coal mine methane by the electrochemical catalysis of sofc anode: from pollutant to clean energy. Appl Catal B-Environ 268:118413. https://doi.org/10.1016/j.apcatb.2019.118413

Wang Y, Lei X, Zhang Y, Chen F, Liu T (2018) In-situ growth of metallic nanoparticles on perovskite parent as a hydrogen electrode for solid oxide cells. J Power Sources 405:114–123. https://doi.org/10.1016/j.jpowsour.2018.10.023

Wang Y, Liu T, Fang S, Chen F (2016a) Syngas production on a symmetrical solid oxide H_2O/CO_2 co-electrolysis cell with $Sr_2Fe_{1.5}Mo_{0.5}O_6$–$Sm_{0.2}Ce_{0.8}O_{1.9}$ electrodes. J Power Sources 305:240–248. https://doi.org/10.1016/j.jpowsour.2015.11.097

Wang Y, Liu T, Lei L, Chen F (2017) High temperature solid oxide H_2O/CO_2 co-electrolysis for syngas production. Fuel Process Technol 161:248–258. https://doi.org/10.1016/j.fuproc.2016.08.009

Wang Y, Liu T, Li M, Xia C, Zhou B, Chen F (2016b) Exsolved Fe–Ni nano-particles from $Sr_2Fe_{1.3}Ni_{0.2}Mo_{0.5}O_6$ perovskite oxide as a cathode for solid oxide steam electrolysis cells. J Mater Chem A 4:14163–14169. https://doi.org/10.1039/c6ta06078a

Wu M, Zhou X, Xu J, Li S, Pan L, Zhang N (2020) Electrochemical performance of $La_{0.3}Sr_{0.7}Ti_{0.3}Fe_{0.7}O_{3-\delta}/CeO_2$ composite cathode for CO_2 reduction in solid oxide electrolysis cells. J Power Sources 451:227334. https://doi.org/10.1016/j.jpowsour.2019.227334

Xie K, Zhang Y, Meng G, Irvine JTS (2011) Direct synthesis of methane from CO_2/H_2O in an oxygen-ion conducting solid oxide electrolyser. Energy Environ Sci 4:2218. https://doi.org/10.1039/c1ee01035b

Xing R, Wang Y, Zhu Y, Liu S, Jin C (2015) Co-electrolysis of steam and CO_2 in a solid oxide electrolysis cell with $La_{0.75}Sr_{0.25}Cr_{0.5}Mn_{0.5}O_{3-\delta}$–Cu ceramic composite electrode. J Power Sources 274:260–264. https://doi.org/10.1016/j.jpowsour.2014.10.066

Yan F, Wang Y, Yang Y, Zhu L, Hu H, Tang Z, Zhang Y, Yan M, Xia C, Xu Y (2020) Distribution of characteristic times: A high-resolution spectrum approach for visualizing chemical relaxation and resolving kinetic parameters of ionic-electronic conducting ceramic oxides. Coatings 10:1240. https://doi.org/10.3390/coatings10121240

Yang Y, Bao H, Ni H, Ou X, Wang S, Lin B, Feng P, Ling Y (2021) A novel facile strategy to suppress sr segregation for high-entropy stabilized $La_{0.8}Sr_{0.2}MnO_{3-\delta}$ cathode. J Power Sources 482:228959. https://doi.org/10.1016/j.jpowsour.2020.228959

Yang Y, Wang Y, Yang Z, Lei Z, Jin C, Liu Y, Wang Y, Peng S (2019) Co-substituted $Sr_2Fe_{1.5}Mo_{0.5}O_{6-\delta}$ as anode materials for solid oxide fuel cells: achieving high performance via nanoparticle exsolution. J Power Sources 438:226989. https://doi.org/10.1016/j.jpowsour.2019.226989

Yaremchenko AA, Macías J, Kovalevsky AV, Arias-Serrano BI, Frade JR (2020) Electrical conductivity and thermal expansion of Ln-substituted $SrTiO_3$ for solid oxide cell electrodes and interconnects: The effect of rare-earth cation size. J Power Sources 474:228531. https://doi.org/10.1016/j.jpowsour.2020.228531

Zhang X, Song Y, Guan F, Zhou Y, Lv H, Wang G, Bao X (2018) Enhancing electrocatalytic CO_2 reduction in solid oxide electrolysis cell with $Ce_{0.9}Mn_{0.1}O_{2-\delta}$ nanoparticles-modified LSGM-GDC cathode. J Catal 359:8–16. https://doi.org/10.1016/j.jcat.2017.12.027

Zhang Y, Yan F, Hu B, Xia C, Yan M (2020) Chemical relaxation in porous ionic–electronic conducting materials represented by the distribution of characteristic times. J Mater Chem A 8:17442–17448. https://doi.org/10.1039/D0TA05613H

Zheng K, Świerczek K, Polfus JM, Sunding MF, Pishahang M, Norby T (2015) Carbon deposition and sulfur poisoning in $SrFe_{0.75}Mo_{0.25}O_{3-\delta}$ and $SrFe_{0.75}Mo_{0.25}O_{3-\delta}$ electrode materials for symmetrical SOFCs. J Electrochem Soc 162:F1078–F1087. https://doi.org/10.1149/2.0981509jes

Zheng Y, Wang J, Yu B, Zhang W, Chen J, Qiao J, Zhang J (2017) A review of high temperature co-electrolysis of H_2O and CO_2 to produce sustainable fuels using solid oxide electrolysis cells (SOECs): advanced materials and technology. Chem Soc Rev 46:1427–1463. https://doi.org/10.1039/C6CS00403B

Zhu J, Zhang W, Li Y, Yue W, Geng G, Yu B (2019) Enhancing CO_2 catalytic activation and direct electroreduction on in-situ exsolved fe/mnox nanoparticles from (Pr, $Ba_)2M_{n2-}yFey_{O5+}\delta$ layered perovskites for SOEC cathodes. Appl Catal B-Environ 268:118389. https://doi.org/10.1016/j.apcatb.2019.118389